Optical Phase-Lock Loop Modeling for WDM System Applications

M. S. Gonçalves and A. C. Bordonalli
State University of Campinas, UNICAMP, Campinas, SP, Brazil

***Abstract* — The transient characteristics of optical phase-lock loops intended for receiver applications in wavelength division multiplexing systems is theoretically analyzed in this work. As the locking bandwidth is controlled by a proper project of the feedback loop, a WDM carrier within the locking range can induce the locking of a slave semiconductor laser and be properly detected without the need for optical filters. The other carriers are discarded by the loop electronics bandwidth. The modeling takes into account the loop feedback effect over the slave laser rate equations, allowing the analysis of the temporal behavior of the locking process. The results show the dynamics of the loop acquisition, considering distinct values of initial frequency difference between carrier and slave laser and different loop filter configurations.**

***Index Terms* — WDM, coherent systems, optical receivers.**

I. Introduction

The evolution of the telecommunication systems has resulted in ideas and projects that combine high capacity and low costs. One way to achieve those is through the use of multiplexing techniques [1] in different physical transmission mediums. After the development of the Erbium doped fiber amplifiers (EDFA), the application of the wavelength division multiplexing (WDM) technique to optical fiber systems became economically possible. In optical WDM, several channels allocated at different optical wavelengths are combined and simultaneously transmitted by an optical fiber, with full access to the fiber bandwidth. Therefore, the system can support high bit rates and offer, at same time, security and reliability.

At the receiver end, the channels need to be isolated for information recovery. Thus, samples of the combined optical signal are filtered by optical filters centered at the different channel carrier frequencies. Unfortunately, the wide bandwidth of these filters is one of the causes for the restriction on the maximum number of transmission channels in WDM systems [1]. Recently, commercial WDM systems can operate with up to 40 channels separated by 100 GHz (~1 nm) from each other [1]. In laboratory, results show that the channel spacing could drop to values slightly below 0.5 nm [2,3].

Aldário C. Bordonalli, aldario@dmo.fee.unicamp.br, and Marcos S. Gonçalves, marcoss@dmo.fee.unicamp.br, are with the Department of Microwave and Optics (DMO), School of Electrical and Computer Engineering (FEEC), State University of Campinas (UNICAMP), Caixa Postal 6101, Campinas, SP, 13081-970, Brazil, tel. +55-19-3788-3704, fax +55-19-3289-1395.

This work was partially supported by CePOF (CEPID-FAPESP), CNPq, CAPES, and FAEP/UNICAMP, Brazil.

The optical phase-lock loop (OPLL) is a feedback optoelectronic circuit that controls the frequency and phase of a local optical source (slave laser - SL) in relation to those of a reference optical source (master laser - ML). Fig. 1 shows the block diagram of a homodyne OPLL. The signals from both lasers are coupled into the photodetector, where they are mixed. The resulting photocurrent is composed by two terms: a DC term, generated by the total optical power reaching the photodetector active area, and an AC error term, produced by the phase and frequency differences between the lasers. The photocurrent is then amplified and processed by the loop filter. When semiconductor lasers are being used, the loop filter output signal is combined with the SL bias current for the SL phase and frequency control.

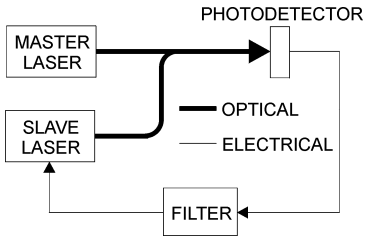

Fig. 1. Block diagram of a homodyne OPLL

Locking can only be achieved if the initial frequency difference between the lasers lies within the so called OPLL acquisition band. Under this condition, during the locking process, the error term magnitude tends to decrease after each feedback cycle as a result of the SL tuning. When locking is acquired, ML and SL operate at same frequency and a residual baseband photocurrent maintains the SL laser frequency displacement in relation to its initial value. The SL laser then responds in tune to any ML frequency fluctuation. However, tracking is lost if the fluctuations exceed the OPLL locking range. As the characteristics of the acquisition and tracking only depend on a proper feedback project, the OPLL locking range can be designed to fulfill different system requirements.

Due to the flexibility in the OPLL locking range design, the OPLL technique can be applied to receivers in WDM systems. In this case, the ML should be considered as one of the WDM channels. If the channel frequency were such that it induced the SL locking, the channel information would be detected and decoded. However, if the frequency difference between the channel and the SL were

outside the acquisition range, the channel would be photodetected but filtered out by the loop electronics. This behavior suggests that a given WDM channel could be selected without the need for optical filters. Therefore, a proper locking bandwidth project could allow the reduction of the WDM channel spacing, resulting in a potential increase in system capacity.

The transient characteristics of optical phase-lock loops intended for receiver applications in wavelength division multiplexing systems are theoretically analyzed in this paper. Firstly, a theoretical study of the OPLL technique is conducted, where the OPLL analysis is adapted to take into account the SL control through the laser rate equations. This approach differs from the traditional OPLL study [4,5]. Following, the simulation results for the transient evolution of the acquisition process of an OPLL are presented, considering two types of loop filters and several initial conditions for the frequency difference between lasers. Also, the effect of the loop propagation delay on the locking performance is investigated.

II. THEORY

The electric fields representing the ML and SL signals can be written as:

$$E_m(t) = E_{mo} e^{j[\omega_m t + \phi_m(t)]} \quad (1a)$$

$$E_s(t) = E_{so} e^{j[\omega_s t + \phi_s(t) + \pi/2]} \quad (1b)$$

where, E_{mo} and E_{so}, ω_m and ω_s, and $\phi_m(t)$ and $\phi_s(t)$ are the electric field amplitudes, the angular frequencies and the phases of the ML and SL, respectively. In a homodyne OPLL, the photodetector is responsible for the optoelectronic conversion and the comparison between the ML and the SL signals (mixing). The latter is properly accomplished when the optical signals are in quadrature ($\pi/2$ rad detune). By assuming the same polarization state for both fields, the total electric field on the photodetector active region is $E_s(t) + E_m(t)$. Thus, the instantaneous photocurrent can be written as [6]:

$$i(t) = K_{co}\{RP_m + RP_s + 2R\sqrt{P_m P_s}\,\mathrm{sen}[\Delta\omega t + \theta(t)]\} \quad (2)$$

where $P_m = A_p E_{mo}^2/2\eta$ and $P_s = A_p E_{so}^2/2\eta$ are the ML and SL average photodetected optical powers, respectively, $\Delta\omega = \omega_m - \omega_s$, $\theta(t) = \phi_m - \phi_s$, η is the characteristic medium impedance, A_p is the photodetector active area, and K_{co} is the photodetector coupling efficiency. In (2), $RP_m + RP_s$ represents the DC photocurrent. However, as both the SL frequency and optical power are controlled by the SL current, the OPLL could misinterpret power oscillations as variations in the phase or frequency difference. Thus, balanced detection is assumed and the DC term discarded.

To consider a more comprehensive OPLL analysis, it is assumed that the photocurrent requires amplification. Thus, the amplifier output voltage is:

$$V_a = G_{amp} Z_{in1}\{K_{co} K_{pd}\,\mathrm{sen}[\Delta\omega t + \theta(t)]\} \quad (3)$$

where G_{amp} is amplifier gain, Z_{in1} is the amplifier input impedance, and $K_{pd} = 2R(P_m P_s)^{1/2}$. The amplifier output signal, V_a, is then coupled into the loop filter. In this paper, two loop filter configurations were considered: the passive modified first order and the active second order filters. Their transfer functions are given, respectively, by:

$$F(s) = \frac{1}{s\tau + 1} \quad (4a)$$

$$F(s) = \frac{s\tau_2 + 1}{s\tau_1} \quad (4b)$$

where τ, τ_1, and τ_2 are time constants. By assuming the filter input impedance as Z_{in2}, the SL controlling current due to the OPLL influence is:

$$i_p(t) = I_p\{\mathrm{sen}[\Delta\omega t + \theta(t)]\} * f(t) \quad (5)$$

where $I_p = G_{amp} Z_{in1} K_{co} K_{pd}/Z_{in2}$ and $f(t)$ is the filter impulse response. Generally, at this point, the OPLL theoretical analysis is simplified [4-6]. The OPLL is assumed to be locked ($\Delta\omega = 0$) and $\theta(t)$ is considered small enough to allow the linearization of (5). In the OPLL modeling presented here, these usual procedures are discarded. As a result, the transient study of the OPLL acquisition and tracking becomes possible and the effect of the feedback loop over the SL behavior can be more realistically observed through the SL rate equations. In this preliminary approach, the reduced form of the semiconductor laser rate equations [7] was adopted for the SL, excluding, for instance, quantum and noise effects. Nevertheless, the use of the simplified rate equations is sufficient to allow conclusions regarding acquisition and tracking bandwidths (locking bandwidths), feedback stability, and cycle slip behavior. The study of other OPLL characteristics requires a more complete set of rate equations and is left for future works. By considering the SL operation beyond threshold, the carrier number rate equation can be written as:

$$\frac{dN}{dt} = \frac{I}{q} - \frac{N}{\tau_e} - GN_{ph} \quad (6)$$

where N is the carrier number, I is the injection current, q is the electron charge, τ_e is the carrier life time, and N_{ph} is the photon number. The relation between the active region gain G and the injected carrier number is assumed to be $G(N) = \Gamma v_g a(N - N_o)$, where Γ is the mode confinement factor, v_g is the modal group velocity, a is the gain constant, and N_o is the transparency carrier number. The photon number rate equation is given by:

$$\frac{dN_{ph}}{dt} = \left(G - \frac{1}{\tau_p}\right)N_{ph} + R_{sp} \quad (7)$$

where τ_p is the photon life time and R_{sp} is the spontaneous emission rate. The phase variation rate is related to the laser injection current through:

$$\frac{d\delta\phi}{dt} = \frac{1}{2}\alpha_{lin}(G - G_o) \tag{8}$$

where α_{lin} is the laser linewidth enhancement factor and G_o is the DC active region gain.

III. Simulation Results

The OPLL simulation routine uses the 4th order Runge-Kutta algorithm to solve the SL rate equations. The ML and SL phases and frequencies are compared by (2). An error signal is generated and its AC part is coupled into the loop filter after amplification. Assuming balanced detection, the DC term is discarded. The filter output signal, given by (5), is then summed to the SL bias current and applied to (6). As a result, the rate equations interact with each other, producing new SL frequency and phase values. Those are compared again with the ML frequency and phase values for a new feedback cycle. The routine is repeated until the error signal tends to a constant value.

For all simulations, the frequency responses of the loop components were assumed ideal, except for those of the loop filters [5,6]. It is intended to avoid this approach in future simulations, as the acquisition in real OPLLs could be seriously compromised. Although this study analyzes particular OPLL transient characteristics for application in WDM receivers, the laser simulation parameters adopted here were for monomode 1.300-nm semiconductor lasers [7]. However, the results could be extended to 1.550 nm without significance loss. The simulation parameters are: $P_m = P_s = 1$ mW, $R = 0.8$ A/W, $\eta = 377\ \Omega$, $K_{co} = 1$, $G_{amp} = 1$, $Z_{in1} = Z_{in2} = 50\ \Omega$, $q = 1.6\times10^{-19}$ C, $\Gamma = 0.3$, $v_g = 7.5\times10^{9}$ cm/s, $a = 2.5\times10^{-16}$ cm^2, $N_o = 1\times10^{8}$, $\tau_e = 2.2$ ns, $\tau_p = 1.6$ ps, the SL bias current $I_o = 20$ mA, $R_{sp} = 1.28\times10^{12}$ s^{-1}, and $\alpha_{lin} = 5$. The total loop gain k was estimated in 7.037×10^{9} rad/s. For a damping ratio ξ_{no} of 0.707, $\tau_1 = 71.3$ ns, $\tau_2 = 4.5$ ns, and $\tau = 71$ ps. The natural angular frequency for the second order loop is $\omega_{no} = 3.14\times10^{8}$ rad/s.

Fig. 2 and 3 show the photocurrent temporal evolution during OPLL locking acquisition for a passive modified first order and an active second order loop filters, respectively. In Fig. 2, the frequency difference between the lasers Δf is 280 MHz. In Fig. 3, $\Delta f = 69$ MHz. It was observed that those two particular values of Δf represented the maximum frequency detunings for which the OPLL acquired lock in one phase transient. In both cases, Δf defines the OPLL lock-in range. A comparison between the simulation and the results from approximate expressions of the lock-in range, $\Delta\omega_l \cong 2\xi_o\omega_{no}$, for second order loops, and $\Delta\omega_l \le k$, for first order loops [4], show reasonable agreement. It is also possible to observe that in both cases, the photocurrent tends to a constant value after locking acquisition. This residual current is necessary to drive the SL and keep its frequency displacement from the free-running value so that locking is ensured. The value of θ necessary to maintain the residual current is known as static phase error. As it can be seen in Fig. 3, for active second order loops, the residual current is considerably small. This characteristic, due to the high DC gain of the active filters, results in an improved noise suppression performance in relation to passive filters.

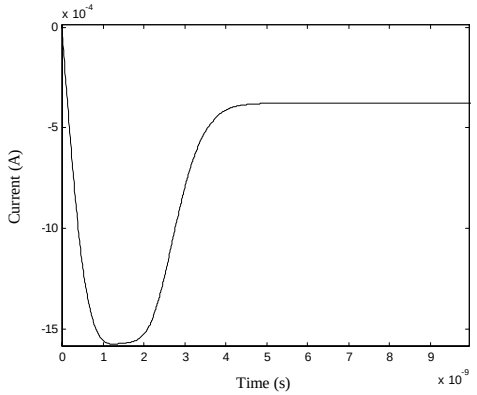

Fig. 2. The photocurrent transient response for the passive modified first order loop inside the lock-in range, initial $\Delta f = 280$ MHz.

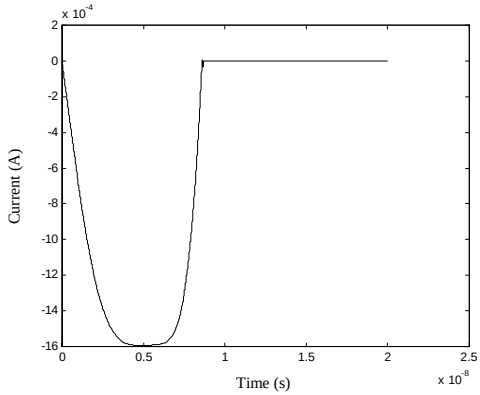

Fig. 3. The photocurrent transient response for the active second order loop inside the lock-in range, initial $\Delta f = 69$ MHz.

Fig. 4 and 5 show the time dependence of Δf during acquisition, for the same simulation parameters as in Fig. 2 and 3, respectively. The initial Δf value corresponds to the lock-in range limit. As the feedback loop controls the slave laser emission, the value of Δf decreases until locking is acquired.

If the frequency difference between the lasers is set to be wider than the lock-in range, the total phase error reaches an absolute critical value of $\pi/2$ rad during acquisition. Due to this phase condition and according to (3), the SL frequency is no longer pulled by the OPLL to match the ML frequency, as the photocurrent reaches its maximum absolute value. However, as time progresses, the total phase error grows beyond $\pi/2$ rad and reduces the photocurrent. As a result, the SL frequency starts to move

back towards its free-running value, suggesting a positive feedback effect. Under these conditions, as time and Δf continuously increase, a minor SL frequency displacement can cause considerable variations in the total phase error value after each OPLL cycle. The negative feedback is restored when the total phase error reaches the next multiple of $\pi/2$ rad. It is important to point out that, at this moment, the instantaneous Δf would be narrower than the initial one as the Δf relation with the total phase error changed with time. The temporary loss of acquisition due to the photodetector phase response is known as cycle slip. The OPLL can acquire lock even with the occurrence of cycles slips, as the instantaneous value of Δf tends to be narrower after each event and, consequently, to fall within the lock-in range. Nevertheless, if the initial value of Δf is excessively wide, locking may never be acquired.

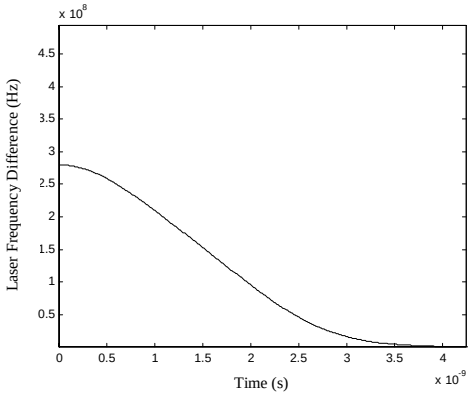

Fig. 4. The laser frequency difference transient response for the passive modified first order loop inside the lock-in range, initial Δf = 280 MHz.

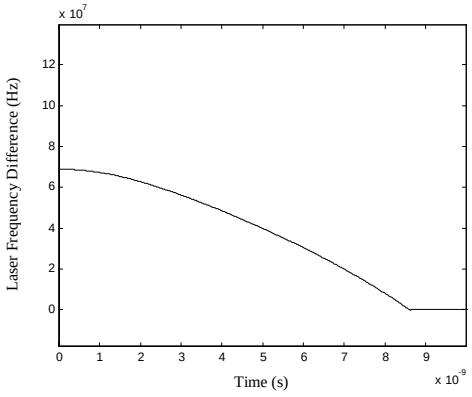

Fig. 5. The transient response of the laser frequency difference for the active second order loop inside the lock-in range, initial Δf = 69 MHz.

Fig. 6 and 7 show the photocurrent transient response during acquisition for a passive modified first order and an active second order loop filters, respectively, when the initial Δf is chosen outside the lock-in range. In Fig. 6, the initial frequency difference between the lasers is 350 MHz. In Fig. 7, the initial Δf = 100 MHz. As acquisition takes place, the OPLL controls the SL in such a way that photocurrent reaches its maximum absolute value K_{pd} = 1.6 mA before locking. At this moment, the total phase error reaches $\pi/2$ rad, forcing a cycle slip. In Fig. 6 and 7, the cycle slip is responsible for the photocurrent oscillation between -1.6 e 1.6 mA. After the cycle slip, the SL frequency is once again pulled towards the ML frequency and locking is achieved with no further cycle slips. It important to mention that both photocurrent transient responses present a DC level, which is responsible to keep the initial SL frequency displacement.

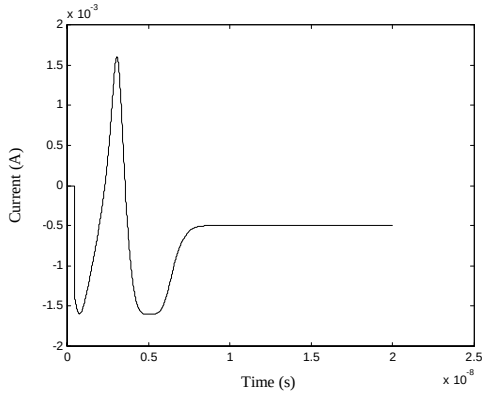

Fig. 6. The photocurrent transient response for the passive modified first order loop outside the lock-in range, initial Δf = 350 MHz.

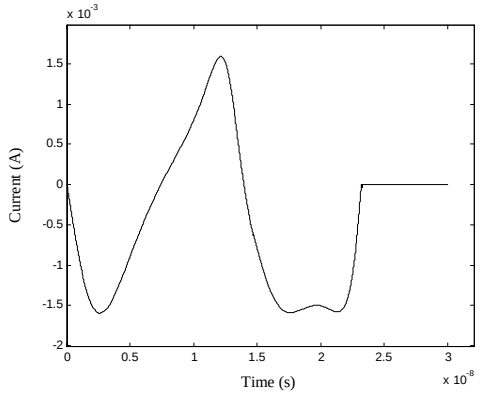

Fig. 7. The photocurrent transient response for the active second order loop outside the lock-in range, initial Δf = 100 MHz.

Fig. 8 e 9 show Δf as a function of the time, for the same simulation parameters as in Fig. 6 and 7, respectively. As the acquisition takes place, Δf is reduced by the feedback control. However, during the cycle slip, Δf increases. When the OPLL recovers the SL frequency pulling, Δf lies already within the lock-in range and lock is acquired with no extra cycle slips.

As mentioned before, an extremely wide initial Δf could prevent locking to happen. The maximum initial value of Δf for which locking can be acquired, even with cycle slipping, is defined as the pull-in range. For the modified first order loop, the pull-in range is given by k [6]. Fig. 10 shows the photocurrent transient response when Δf = 1.12 GHz and the SL free-running frequency > the ML one.

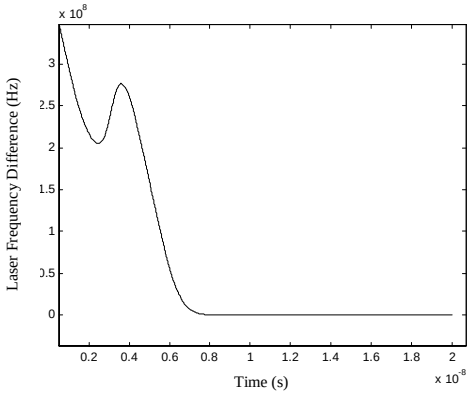

Fig. 8. The laser frequency difference transient response for the passive modified first order loop outside the lock-in range, initial Δf = 350 MHz.

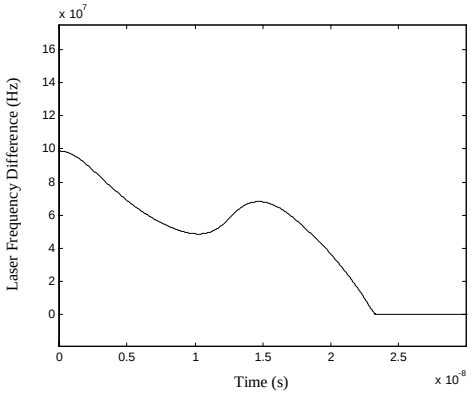

Fig. 9. The transient response of the laser frequency difference for the active second order loop outside the lock-in range, initial Δf = 100 MHz.

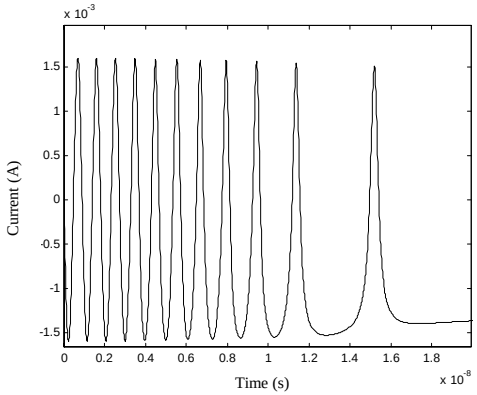

Fig. 10. The photocurrent transient response for the passive modified first order loop inside the pull-in range, initial Δf = 1.12 GHz.

For a wide initial Δf, the loop filter attenuates the SL controlling signal and Δf varies slowly. Cycle slips occur, given the photocurrent the initial sinusoidal-like shape. Yet, the curve presents a small DC content to keep the SL laser frequency variation. As Δf approaches the lock-in range, the curve becomes more asymmetric, increasing the DC content and resulting in a more efficient SL frequency pulling. Even with cycle slips, the OPLL tends to acquire locking after few more OPLL cycles. Fig. 11 shows the time dependence of Δf during acquisition for the same simulation parameters as in Fig. 10. The slow initial variation of Δf is readily seen.

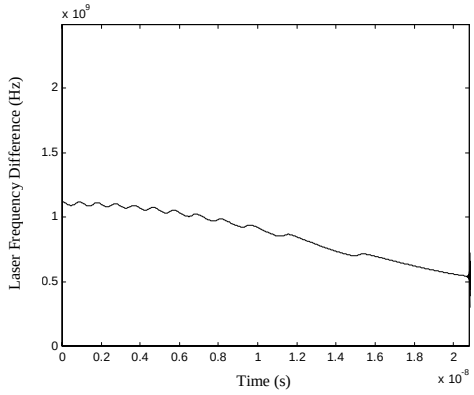

Fig. 11. The laser frequency difference transient response for the passive modified first order loop inside the pull-in range, initial Δf = 1.12 GHz.

For initial Δf values wider than the pull-in range, the loop gain is insufficient to provide enough current to control the SL frequency. The OPLL presents only a cycle slipping behavior and the photocurrent oscillates continuously. Fig. 12 shows the photocurrent for such a situation, where Δf = 2.8 GHz.

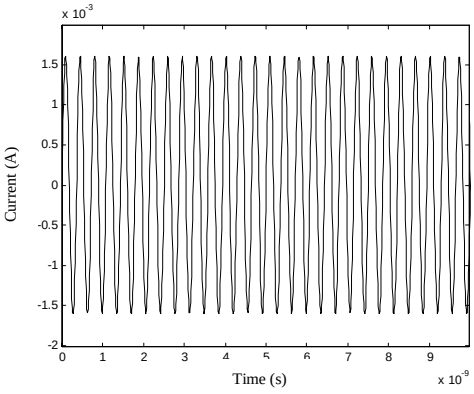

Fig. 12. The photocurrent transient response for the passive modified first order loop outside the pull-in range, initial Δf = 2.8 GHz.

In the case of ideal active second order loops, the pull-in range tends to the infinity [4] as a result of the large loop DC gain. In other words, whatever the initial Δf is, the OPLL is already in acquisition. In real systems, however, as the loop component characteristics are considered, the pull-in becomes limited to finite values. Fig. 13 shows the photocurrent transient response during acquisition for an ideal active second order loop filter, for initial Δf = 400 MHz and the ML free-running frequency > the SL one. The latter cause an inversion in the asymmetric pattern of the curve in relation to that of the Fig. 10. Nevertheless, the same conclusions as those for the modified first order loop are valid in this case.

So far, the loop delay influence has been neglected. However, the overall OPLL performance strongly depends

on the delay introduced by the loop electronics and the optical and electrical paths. Table I lists the lock-in range results for the modified first order (MFO) and active second order (ASO) loop filters, when the loop delay T_d is 1, 2, and 3 ns. The delay effect is added to the analysis by applying the convolution of (5) with respect to e^{-T_d}.

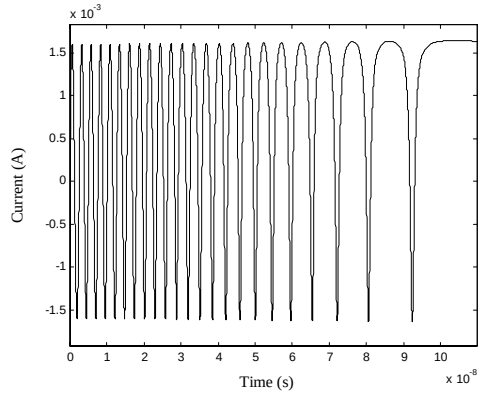

Fig. 13. The photocurrent transient response for the active second order loop outside the lock-in range, initial Δf = 400 MHz.

By comparison, the MFO lock-in range is seen to be more sensitive to the influence of T_d then that of the ASO, suffering stronger range reduction in relation to the zero-delay case. In general terms, these results suggest that OPLLs will tend to loose their acquisition and tracking abilities for longer values of loop delay. Fig. 14 e 15 show the photocurrent transient response, respectively, for the passive MFO loop filter, with T_d = 10 ns and Δf = 4 MHz, and the ASO loop filter, with T_a = 20 ns and Δf = 20 MHz. In both situations, the initial Δf would be well within the non-delay lock-in range. However, the delay effect prevents locking as even the pull-in range condition is violated by the values of delay considered.

TABLE I LOOP DELAY AND THE LOCK-IN RANGE

T_d	$\Delta\omega_l$ - MFO	Reduction	$\Delta\omega_l$ - ASO	Redução
1 ns	124 MHz	55,7%	61 MHz	11,5%
2 ns	30 MHz	89,2%	52 MHz	24,6%
3 ns	4 MHz	98,5%	41 MHz	40,5%

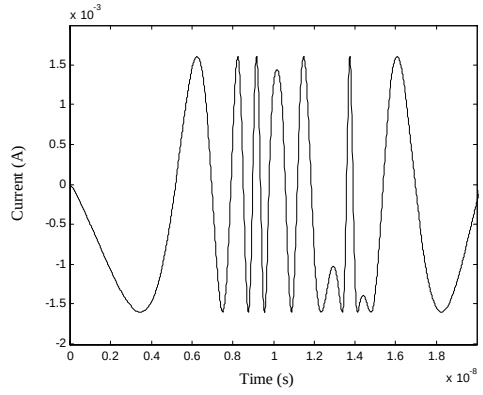

Fig. 14. The photocurrent transient response for the passive modified first order loop outside the pull-in range, initial Δf = 4 GHz, T_d = 10 ns.

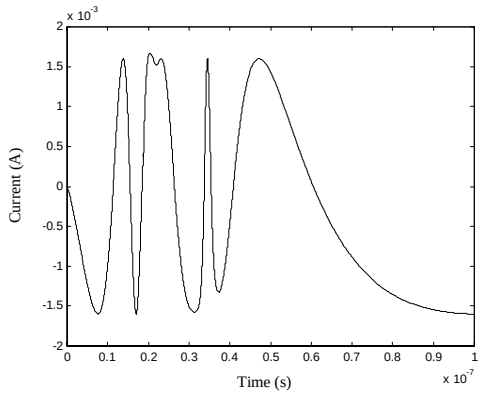

Fig. 15. The photocurrent transient response for the active second order loop outside the pull-in range, initial Δf = 4 GHz, T_d = 10 ns.

IV. CONCLUSIONS

The OPLL transient characteristics for WDM receiver applications were theoretically analyzed in this work. For WDM systems, only one channel induces locking. The others are filtered out by the loop bandwidth, reducing the need for optical filters. As the OPLL locking bandwidth depends only on a proper feedback design, the WDM channel spacing could be made narrower as required. For the loop filters adopted, the zero-delay OPLL locking behavior was observed for different Δf situations: inside the lock-in and pull-in ranges, and outside the acquisition. The results are in agreement with those of previous works. The loop delay effect was also considered. In general, the acquisition ranges became narrower for both types of filter, suggesting that locking could be prevented for longer time delay values. Future works should consider the transient analysis of other OPLL characteristics such as stability and noise suppression and their relation with the loop delay.

REFERENCES

[1] R. Ramaswami e K. N. Sivarajan, "Optical Networks – A Practical Perspective", Morgan Kaufmann, San Francisco, USA, 1998.

[2] J. J. Pan e Y. Shi: "Bandwidth reduction technique for multiplayer wavelength division multiplexing (WDM) bandpass filters", *Electron. Lett.*, *v*ol. 34, no. 1, 1998.

[3] J. D. T. Kruschwitz: "Bandwidth reduction technique for multilayer wavelength division multiplexing (WDM) bandpass filters", *Appl. Opt.*, *v*ol. 39, no. 34, 2000.

[4] L. G. Kazovsky e D. A. Atlas: "A 1320-nm experimental optical phase-locked loop: Performance investigation and PSK homodyne experiments at 140 Mb/s and 2 Gb/s", *J. Ligthwave Technol.* vol. 8, no. 9, 1990.

[5] R. T. Ramos e A. J. Seeds: "Comparison between first order and second order optical phase-lock loops", *IEE Microw. Guided Wave Lett.*, vol. 4, no. 1, 1994.

[6] A. C. Bordonallli, C. Walton e A. J. Seeds: "High-performance phase locking of wide linewidth semiconductor lasers by combined use of injection locking and optical phase-lock-loop", *J. Ligthwave Technol.* vol. 17, no. 2, 1999.

[7] G. P. Agrawal e N. K. Dutta: "Semiconductor Lasers", 2nd edition, Van Nostrand Reinhold, New York, USA, 1993.